Steady-State Analysis of the Modular Multilevel Converter

Daniel Westerman Spier
and Joaquim López Mestre
CINERGIA
Control Intel·ligent de l'Energia, SCCL
Badalona, Spain
daniel.westerman@cinergia.coop
quimlopez@cinergia.coop

Eduardo Prieto-Araujo
and Oriol Gomis-Bellmunt
CITCEA
Universitat Politècnica de Catalunya (UPC)
Barcelona, Spain
eduardo.prieto-araujo@citcea.upc.edu
gomis@citcea.upc.edu

Abstract

In this paper, the steady-state behavior of the modular multilevel converter (MMC) is studied under balanced and unbalanced AC grid voltage conditions. The suggested mathematical model is derived combining the converter internal arm variables and both AC and DC grids variables. Moreover, the steady-state solution of the system can be achieved by setting the internal power balance within the converter. In order to verify the steady-state model, different types of AC fault conditions are imposed, and the output values are compared with the simulation results of an average model of the MMC circuit. The results show that the proposed analysis is in close agreement with the simulations for all conditions evaluated, validating the developed equations.

Index Terms

HVDC, MMC, steady-state analysis, unbalanced voltage sags.

I. Introduction

Modular Multilevel Converter are the preferred choice for modern High Voltage DC (HVDC) transmission systems [1]- [3]. Firstly introduced by [4], the MMC can output high quality voltage waveforms with low harmonic content while switching at low frequency [5], [6]. Previous works have been carried out to describe the steady-state behavior of the MMC when it is operated under balanced AC network conditions [7]–[9].

In order to improve the mathematical description of the system under unbalanced AC voltage conditions, different papers have been proposed [10]–[13]. These articles are based on additive and differential magnitudes to simplify the understanding of the steady-state behavior of the converter. Nevertheless, the usage of the aforementioned variables does not allow observing the individual phase quantities, and consequently, it cannot predict when such values are exceeding the converter limits. Another approach to describe the steady-state behavior of the MMC was introduced by [14]. However, this model only considers a single type of fault and requires the addition of a DC load impedance to attenuate the oscillations in the DC bus caused by the zero sequence current component.

Therefore, a steady-state model that represents all the MMC components separately for any AC network condition and removes the potential circulation of zero sequence current components completely from the model can provide useful insights. In this paper, the steady-state mathematical model of the MMC is derived in the *abc* reference frame, considering all the degrees of freedom of the converter. The analysis is performed by decoupling the AC and DC magnitudes, giving the bases to obtain the MMC upper and lower arm voltages, currents and powers. To validate the suggested model, several types of AC voltage sags are imposed into the steady-state equations, and the time and phasor domains responses are compared with an average model of the MMC circuit simulated in Matlab Simulink®. The results confirm that the proposed model has the same behavior as the MMC simulation model for all the different AC grid scenarios considered.

This paper is organized as follows. In Section I the introduction was given. Section II presents the description of the system. The steady-state mathematical description of the MMC is presented in Section III, while Section IV shows the summary of the complete model. The simulation results are displayed in Section V. Finally, the conclusions are discussed in Section VI.

II. System description

The three-phase MMC consists of three legs, one per phase, in which each leg has two stacks of N_{arm} half-bridge sub-modules, known as the upper and lower arms. The complexity of the sub-modules can vary according to the application [15]. In this article, the half-bridge topology is chosen as it is widely used in the industry.

In Fig. 1, the converter variables are described as follows: u_g^k is the AC network voltage, u_u^k and u_l^k are the upper and lower arms voltages respectively, U_u^{DC} and U_l^{DC} are the upper and lower DC grid voltages, i_u^k and i_l^k are the upper and lower arm currents respectively, i_s^k is the AC network current, R_a and L_a are the arm impedances and finally, R_s and L_s are the phase reactor impedances. The steady-state equations are derived considering a generic AC network, that can be either balanced

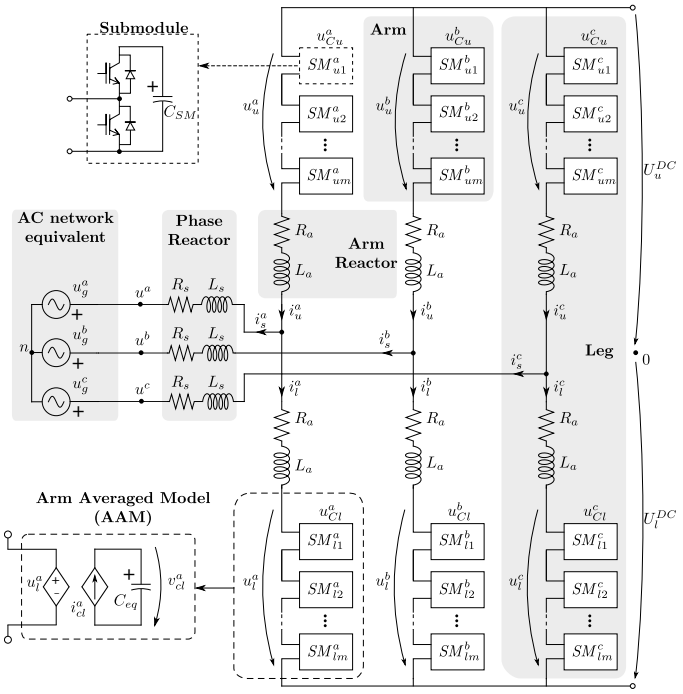

Fig. 1. Complete model of the MMC converter.

or unbalanced. In addition, the MMC variables contain both AC and DC components, which are decoupled to simplify the derivation process. Thus, separating the AC and DC elements, the arms' voltages and currents can be calculated and further used to establish the converter internal energy balanced condition.

The parameters for the HVDC system are given in Table I. Based on these values, all the system variables can be described and the steady-state condition of the MMC in the *abc* reference frame can be obtained.

TABLE I
SYSTEM PARAMETERS

Parameter	Symbol	Value	Units
Rated power	S	526	MVA
Rated power factor	$\cos\phi$	0.95 (c)	-
AC-side voltage	U_g	320	kV rms ph-ph
HVDC link voltage	U^{DC}	$\pm$320	kV
Phase reactor impedance	Z_s	j 0.05	pu
Arm reactor impedance	Z_a	0.01+j 0.2	pu
Converter modules per arm	N_{arm}	400	-
Average module voltage	V_{module}	1.6	kV
Sub-module capacitance	C_{module}	8	mF

III. STEADY-STATE MODEL DERIVATION

In this section the steady-state mathematical model of the converter is derived in the *abc* reference frame.

A. AC grid analysis

For the AC analysis, the DC network is short-circuited; thus, zero DC voltage is applied. Moreover, the AC variables are expressed in the complex domain, defining their real and imaginary parts as

$$\underline{X}_y^k = X_{y_r}^k + jX_{y_i}^k \tag{1}$$

where the $\underline{X}_y^k$ represents any complex term of the MMC, subscripts *r* and *i* represent the real and imaginary part of the variables, respectively, and the superscript k represents the grid phases, with $k \in \{a, b, c\}$.

B. AC grid current calculation

Based on the active P^{k*} and reactive Q^{k*} power references in each of the three phases, the grid current for balanced or unbalanced AC grid conditions can be calculated as

$$\underline{I}_{s_o}^k = \left(\frac{\underline{S}^k}{\underline{U}_g^k}\right)^* \tag{2}$$

with $\underline{I}_{s_0}^k$ as the phasor for the original phase grid current. During unbalanced AC voltage sags, the calculation of $\underline{I}_{s_0}^k$ may have zero sequence components. However, the system has a three-wire connection in the AC side and consequently, the zero sequence current component must be strictly zero. Thus, to eliminate the zero sequence current component in the steady-state model, the original grid current must firstly be decomposed into positive, negative and zero sequence components using Fortescue transformation, as

$$\mathbf{\Theta}^{+-0} \triangleq \mathbf{F} \cdot \mathbf{\Theta}^{abc} = \frac{1}{3}\begin{bmatrix} 1 & \underline{p}^2 & \underline{p} \\ 1 & \underline{p} & \underline{p}^2 \\ 1 & 1 & 1 \end{bmatrix} \cdot \mathbf{\Theta}^{abc} \tag{3}$$

with $\underline{p} = e^{j\frac{-2\pi}{3}}$. Afterwards, to remove the zero sequence component from the original grid current, the steps presented in (4) must be followed.

$$\begin{aligned} \mathbf{I}_s^{abc} &= \mathbf{F}^{-1} \cdot \begin{bmatrix} 1 & 0 & 0 \\ 0 & 1 & 0 \\ 0 & 0 & 0 \end{bmatrix} \cdot \mathbf{F} \cdot \mathbf{I}_{s_o}^{abc} \\ \mathbf{I}_s^{abc} &= \frac{1}{3}\begin{bmatrix} 2 & -1 & -1 \\ -1 & 2 & -1 \\ -1 & -1 & 2 \end{bmatrix} \cdot \mathbf{I}_{s_o}^{abc} \end{aligned} \tag{4}$$

in which $\mathbf{I}_s^{abc}$ is the phase grid current vector without the zero sequence component. Both the grid voltage $\underline{U}_g^k$ and the obtained AC grid current $\underline{I}_s^{abc}$ are used as inputs of the suggested steady-state model (see Section IV).

C. AC MMC equations

In order to build the steady-state model, basic MMC circuit equations must be derived. By applying Kirchhoff Voltage Law (KVL) in the converter and imposing zero DC voltage, the AC voltage equations for the upper and lower arms can be described as

$$\underline{U}_{0n} = \underline{U}_g^k + \underline{Z}_s(\underline{I}_u^k - \underline{I}_l^k) + \underline{Z}_a\underline{I}_u^k + \underline{U}_u^k \tag{5}$$

$$\underline{U}_{0n} = \underline{U}_g^k + \underline{Z}_s(\underline{I}_u^k - \underline{I}_l^k) - \underline{Z}_a\underline{I}_l^k - \underline{U}_l^k \tag{6}$$

where, $\underline{U}_{0n}$ is the voltage difference between the converters DC reference node and the neutral of the AC three-phase system.

In addition to the previous KVL six equations, the equations relating the AC network current $\underline{I}_s^k$ and the arm currents $\underline{I}_u^k$ and $\underline{I}_l^k$ can be obtained using Kirchhoff current law (KCL) in the middle point of the MMC arms, as

$$\underline{I}_s^k = \underline{I}_u^k - \underline{I}_l^k \tag{7}$$

Furthermore, the circulation of AC current through the DC network must be avoided. This restriction can be met by imposing that the sum of the upper arms current is equal to zero, as

$$\underline{I}_u^a + \underline{I}_u^b + \underline{I}_u^c = 0 \tag{8}$$

It should be considered that no additional equation is required to eliminate the zero sequence current component in the lower arms, since it can be directly obtained by combining the equations (7) and (8), which are already part of the model.

The last equations to be included in the AC analysis aim to achieve the steady-state conditions by imposing that the active and reactive powers exchanged between the upper and lower arms are equal, expressed as

$$P_u^k = P_l^k \rightarrow U_{u_r}^k I_{u_r}^k + U_{u_i}^k I_{u_i}^k = U_{l_r}^k I_{l_r}^k + U_{l_i}^k I_{l_i}^k \tag{9}$$

$$Q_u^k = Q_l^k \rightarrow U_{u_r}^k I_{u_i}^k - U_{u_i}^k I_{u_r}^k = U_{l_r}^k I_{l_i}^k - U_{l_i}^k I_{l_r}^k \tag{10}$$

In summary, the AC modelling part consists of the equation set (5)-(10), including the grid voltage $\underline{U}_g^k$ and the AC current $\underline{I}_s^k$ as inputs. Also, P^{k*} and Q^{k*} should be considered as necessary inputs since they are used to calculate $\underline{I}_s^k$.

D. DC analysis of the MMC

For the DC analysis, an analogous procedure to the AC analysis can be performed. Now, only DC voltage is applied to the system while the three-phase AC voltage is set to be zero. Consequently, purely DC current components will be flowing through the MMC. Then, KVL can be applied internally within the converter phase branches and the DC bus, obtaining

$$U^{DC} = U_u^{kDC} + U_l^{kDC} + 2R_a I^{kDC} \tag{11}$$

In addition, the total DC current of the system can be obtained applying KCL to the positive pole of the converter, yielding

$$I_{tot}^{DC} = I^{aDC} + I^{bDC} + I^{cDC} \tag{12}$$

where I^{kDC} is the DC current for each phase and I_{tot}^{DC} is the total DC current flowing through the system.

Therefore, the DC modelling stage consists of the equation set (11) and (12), also including the DC grid voltage U^{DC} as an input parameter of the model.

E. Steady-state power balance equations

In steady-state conditions, the AC and DC active power exchanged in each of the arms should be equal, if the semi-conductor losses are neglected. Obviously, this is not feasible with instantaneous values (as AC power is non-constant). However, it is possible to impose an equality between the AC average power (calculated in the phasor domain) and the DC power. If this condition is not achieved, the energy in the arms cells would either charge or discharge the arm capacitors and therefore, steady-state conditions would not hold. This constraint can be mathematically expressed as,

$$P_u^{kAC} = P_u^{kDC} \rightarrow U_{u_r}^k I_{u_r}^k + U_{u_i}^k I_{u_i}^k = U_u^{kDC} I^{kDC} \tag{13}$$

$$P_l^{kAC} = P_l^{kDC} \rightarrow U_{l_r}^k I_{l_r}^k + U_{l_i}^k I_{l_i}^k = U_l^{kDC} I^{kDC} \tag{14}$$

As a result, the power balance equations (13) and (14) must be included into the model. With the addition of those terms, the steady-state mathematical model of the MMC is completed.

IV. Complete model

The full non-linear steady-state model for all the three-phase, (consider that $k \in \{a, b, c\}$), can be summarized as,

- 13 given real input parameters: $(P^{k*}, Q^{k*}, \underline{U}_g^k, \underline{I}_s^k, U^{DC})$
- 36 real variables given as:
  - 13 complex AC variables: $(\underline{U}_{u,l}^k, \underline{I}_{u,l}^k, \underline{U}_{0n})$
  - 10 real DC variables: $(U_{u,l}^{kDC}, I^{kDC}, I_{tot}^{DC})$
- 36 real equations divided as:
  - 20 complex linear AC equations,

$$\begin{cases} \underline{U}_{0n} = \underline{U}_g^k + \underline{Z}_s(\underline{I}_u^k - \underline{I}_l^k) + \underline{Z}_a \underline{I}_u^k + \underline{U}_u^k \\ \underline{U}_{0n} = \underline{U}_g^k + \underline{Z}_s(\underline{I}_u^k - \underline{I}_l^k) - \underline{Z}_a \underline{I}_l^k - \underline{U}_l^k \\ \underline{I}_s^k = \underline{I}_u^k - \underline{I}_l^k \\ 0 = \underline{I}_u^a + \underline{I}_u^b + \underline{I}_u^c \end{cases} \tag{15}$$

  - 4 linear DC equations,

$$\begin{cases} U^{DC} = U_u^{kDC} + U_l^{kDC} + 2R_a I^{kDC} \\ I_{tot}^{DC} = I^{aDC} + I^{bDC} + I^{cDC} \end{cases} \tag{16}$$

  - 12 non-linear equations,

$$\begin{cases} U_{u_r}^k I_{u_r}^k + U_{u_i}^k I_{u_i}^k = U_{l_r}^k I_{l_r}^k + U_{l_i}^k I_{l_i}^k \\ U_{u_r}^k I_{u_i}^k - U_{u_i}^k I_{u_r}^k = U_{l_r}^k I_{l_i}^k - U_{l_i}^k I_{l_r}^k \\ U_{u_r}^k I_{u_r}^k + U_{u_i}^k I_{u_i}^k = U_u^{kDC} I^{kDC} \\ U_{l_r}^k I_{l_r}^k + U_{l_i}^k I_{l_i}^k = U_l^{kDC} I^{kDC} \end{cases} \tag{17}$$

The mathematical model was developed considering a constant active P^{k*} and reactive Q^{k*} power references (used to calculate the current input $\underline{I}_s^k$). Since both active and reactive powers inputs are introduced per phase into the model, different conditions can be imposed such as positive sequence control, for example. To do so, the negative sequence components of the grid voltages and currents must be eliminated using (3) before adding those variables into the model. The removal of the zero sequence component of the grid current must be maintained as before by employing (4). However, the other stages of the steady-state model given by (5) to (14) are the same.

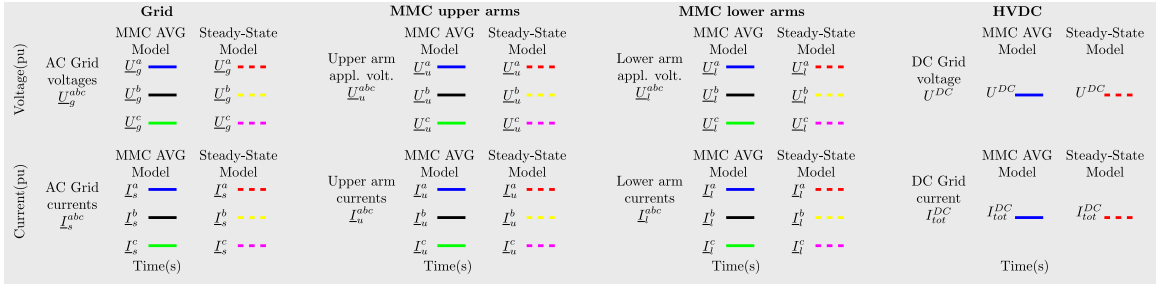

Fig. 2. Simulation results of the MMC operation. Graphs detailed legend.

V. Simulation Results

To validate the proposed mathematical model, the time and phasor domains responses are compared with an average MMC circuit for balanced condition and for the seven different types of voltage sags [16]. For every faulty condition, the value of the faulted phase was set to 0.33 p.u. The variables of interest are displayed according to Fig. 2. In Fig. 3, the time-domain steady-state behavior of the three-phase voltages and currents of the AC network and the MMC upper and lower arms together with the HVDC side variables are shown.

As aforementioned, the steady-state model assumes that the power for each phase is constant for every AC grid voltage condition. Examining Fig. 3, it is clear that to meet this requirement, the MMC circuit must inject different current levels for each phase, depending on the AC voltage sag type, in order to maintain the same power level for the three-phase system. Although these currents present different magnitudes, their sum is strictly zero, as no zero sequence current component circulates through the converter. Furthermore, the steady-state model is able to predict all the different steady-state behaviors of the MMC circuit for the different voltage sags imposed.

In Tables II and III, given in the Appendix A, the phasor values for the balanced and unbalanced grid conditions are shown. The phasors' magnitudes are expressed per unit, which are obtained using the system parameters from Table I as the base values, whereas the angles are displayed in radians. Moreover, the Sim values are obtained from the MMC circuit, while the Mod ones are collected from the steady-state equations. Observing the values from Tables III and IV, it can be stated that the mathematical model and the MMC circuit variables are in close agreement for any voltage sag.

VI. Conclusion

In this paper, a steady-state mathematical model of the MMC was derived to calculate the system magnitudes in balanced and unbalanced AC network voltage conditions. The suggested approach allows all the MMC variables to be analyzed per component and in the abc domain. Therefore, the behavior of the converter can be fully reproduced.

To validate the analysis, different types of faults were employed into the model and compared to an average model of the MMC circuit. The results have shown that the model can fully describe the performance of the converter, for any AC voltage sag condition, validating the steady-state model.

Acknowledgments

This project has received funding from the European Union's Horizon 2020 research and innovation programme under the Marie Sklodowska-Curie grant agreement no. 765585. This document reflects only the authors views; the European Commission is not responsible for any use that may be made of the information it contains. This work was partially supported by the Spanish Ministry of Science, Innovation and Universities under the Project RTI2018-095429-B-I00. This work was co-financed by the European Regional Development Fund. E. Prieto is lecturer of the Serra Húnter Programme.

References

[1] D. Van Hertem, O. Gomis-Bellmunt, and J. Liang, *HVDC Grids: For Offshore and Supergrid of the Future*, ser. IEEE Press Series on Power Engineering. Wiley, 2016.

[2] E. Prieto-Araujo, A. Junyent-Ferré, G. Clariana-Colet, and O. Gomis-Bellmunt, "Control of modular multilevel converters under singular unbalanced voltage conditions with equal positive and negative sequence components," *IEEE Transactions on Power Systems*, vol. 32, no. 3, pp. 2131–2141, May 2017.

[3] E. Sánchez-Sánchez, E. Prieto-Araujo, A. Junyent-Ferré, and O. Gomis-Bellmunt, "Analysis of mmc energy-based control structures for vsc-hvdc links," *IEEE Journal of Emerging and Selected Topics in Power Electronics*, vol. 6, no. 3, pp. 1065–1076, Sep. 2018.

[4] A. Lesnicar and R. Marquardt, "An innovative modular multilevel converter topology suitable for a wide power range," in *2003 IEEE Bologna Power Tech Conference Proceedings,*, vol. 3, June 2003, p. 6 pp. Vol.3.

[5] O. C. Sakinci and J. Beerten, "Generalized dynamic phasor modeling of the mmc for small-signal stability analysis," *IEEE Transactions on Power Delivery*, vol. 34, no. 3, pp. 991–1000, June 2019.

[6] M. Priya, P. Ponnambalam, and K. Muralikumar, "Modular-multilevel converter topologies and applications a review," *IET Power Electronics*, vol. 12, no. 2, pp. 170–183, 2019.

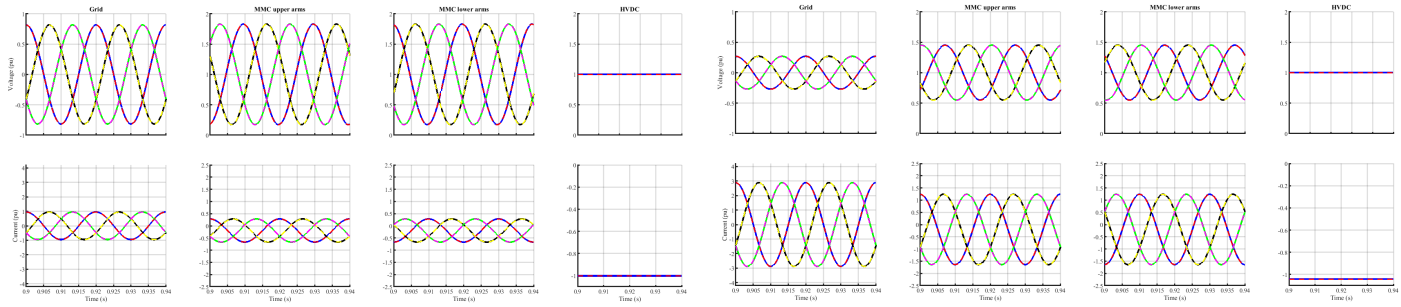

(a) Balanced AC network

(b) Fault type A

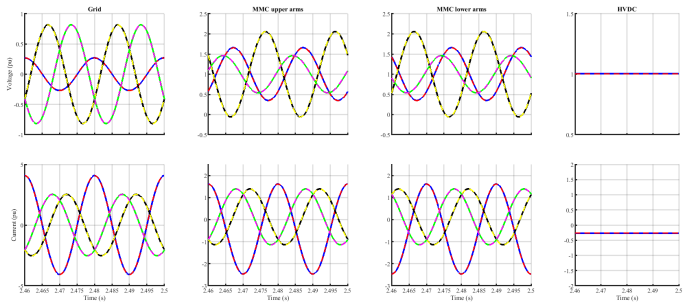

(c) Fault type B

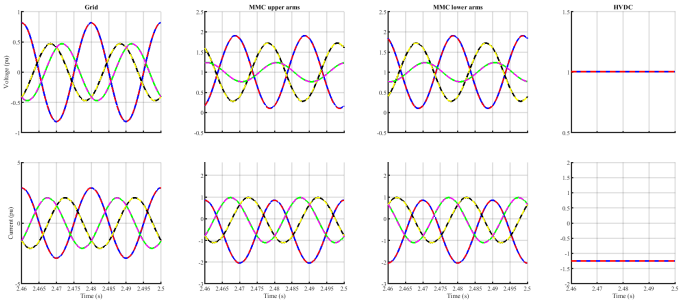

(d) Fault type C

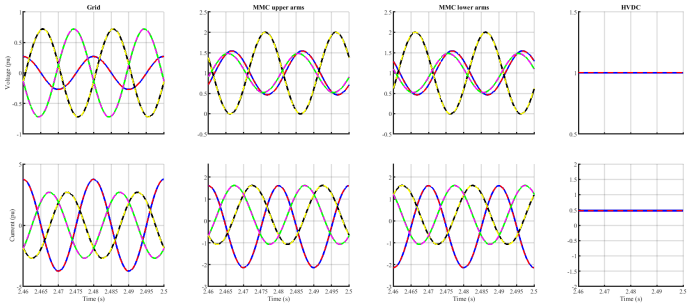

(e) Fault type D

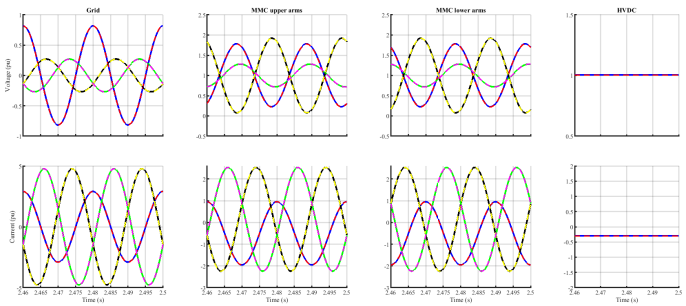

(f) Fault type E

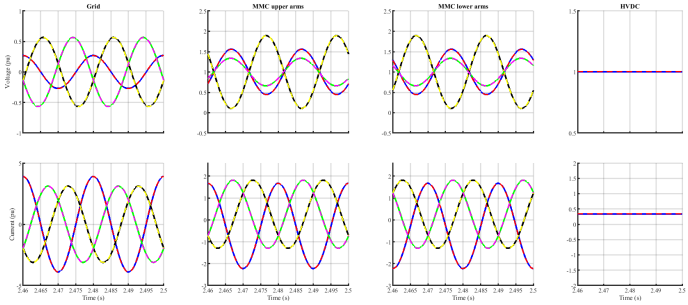

(g) Fault type F

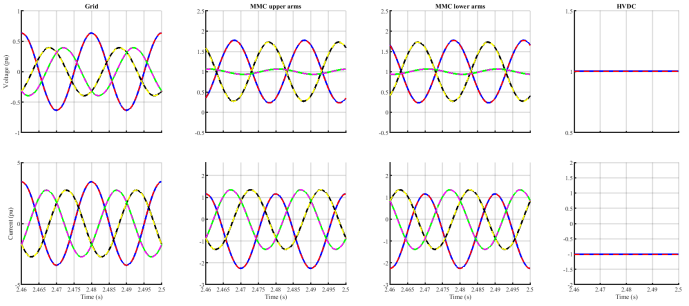

(h) Fault type G

Fig. 3. Time-domain voltages and currents of the AC grid, MMC upper and lower arms and, HVDC grid.

[7] S. Norrga, L. Ängquist, K. Ilves, L. Harnefors, and H. Nee, "Decoupled steady-state model of the modular multilevel converter with half-bridge cells," in *6th IET International Conference on Power Electronics, Machines and Drives (PEMD 2012)*, March 2012, pp. 1–6.
[8] K. Ilves, A. Antonopoulos, S. Norrga, and H. Nee, "Steady-state analysis of interaction between harmonic components of arm and line quantities of modular multilevel converters," *IEEE Transactions on Power Electronics*, vol. 27, no. 1, pp. 57–68, Jan 2012.
[9] Q. Song, W. Liu, X. Li, H. Rao, S. Xu, and L. Li, "A steady-state analysis method for a modular multilevel converter," *IEEE Transactions on Power Electronics*, vol. 28, no. 8, pp. 3702–3713, Aug 2013.
[10] M. Saeedifard and R. Iravani, "Dynamic performance of a modular multilevel back-to-back hvdc system," *IEEE Transactions on Power Delivery*, vol. 25, no. 4, pp. 2903–2912, Oct 2010.
[11] M. Guan and Z. Xu, "Modeling and control of a modular multilevel converter-based hvdc system under unbalanced grid conditions," *IEEE Transactions on Power Electronics*, vol. 27, no. 12, pp. 4858–4867, Dec 2012.
[12] J. Wang, J. Liang, C. Wang, and X. Dong, "Circulating current suppression for mmc-hvdc under unbalanced grid conditions," *IEEE Transactions on Industry Applications*, vol. 53, no. 4, pp. 3250–3259, July 2017.
[13] Q. Tu, Z. Xu, Y. Chang, and L. Guan, "Suppressing dc voltage ripples of mmc-hvdc under unbalanced grid conditions," *IEEE Transactions on Power Delivery*, vol. 27, no. 3, pp. 1332–1338, July 2012.
[14] X. Shi, Z. . Wang, B. Liu, Y. Li, L. M. Tolbert, and F. Wang, "Steady-state modeling of modular multilevel converter under unbalanced grid conditions," *IEEE Transactions on Power Electronics*, vol. 32, no. 9, pp. 7306–7324, Sep. 2017.
[15] K. Sharifabadi, L. Harnefors, H. P. Nee, S. Norrga, and R. Teodorescu, *Design, Control and Application of Modular Multilevel Converters for HVDC Transmission Systems*. Wiley-IEEE press, 2016.
[16] M. Bollen and L. Zhang, "Different methods for classification of three-phase unbalanced voltage dips due to faults," *Electric Power Systems Research*, vol. 66, no. 1, pp. 59 – 69, 2003.

APPENDIX A - MODEL VALIDATION

TABLE II
BALANCED AND FAULT COMPARISON (PART I)

Parameters	**AC grid condition**							
	Balanced		Fault A		Fault B		Fault C	
	Sim	Mod	Sim	Mod	Sim	Mod	Sim	Mod
$\underline{U}_g^a$	$0.8\angle\underline{0}$	$0.8\angle\underline{0}$	$0.27\angle\underline{0}$	$0.27\angle\underline{0}$	$0.3\angle\underline{0}$	$0.3\angle\underline{0}$	$0.8\angle\underline{0}$	$0.8\angle\underline{0}$
$\underline{U}_g^b$	$0.8\angle\underline{-2.1}$	$0.8\angle\underline{-2.1}$	$0.27\angle\underline{-2.1}$	$0.27\angle\underline{-2.1}$	$0.5\angle\underline{-2.6}$	$0.5\angle\underline{-2.6}$	$0.5\angle\underline{-2.6}$	$0.5\angle\underline{-2.6}$
$\underline{U}_g^c$	$0.8\angle\underline{-4.2}$	$0.8\angle\underline{-4.2}$	$0.27\angle\underline{-4.2}$	$0.27\angle\underline{-4.2}$	$0.8\angle\underline{-4.2}$	$0.8\angle\underline{-4.2}$	$0.5\angle\underline{-3.7}$	$0.5\angle\underline{-3.7}$
$\underline{I}_s^a$	$0.95\angle\underline{0}$	$0.95\angle\underline{0}$	$2.88\angle\underline{0}$	$2.88\angle\underline{0}$	$4.1\angle\underline{0}$	$4.1\angle\underline{0}$	$2.9\angle\underline{0}$	$2.9\angle\underline{0}$
$\underline{I}_s^b$	$0.95\angle\underline{-2.09}$	$0.95\angle\underline{-2.09}$	$2.88\angle\underline{-2.09}$	$2.88\angle\underline{-2.09}$	$2.5\angle\underline{-3.8}$	$2.5\angle\underline{-3.8}$	$2.1\angle\underline{-3.9}$	$2.1\angle\underline{-3.9}$
$\underline{I}_s^c$	$0.95\angle\underline{-4.19}$	$0.95\angle\underline{-4.19}$	$2.88\angle\underline{-4.19}$	$2.88\angle\underline{-4.19}$	$2.5\angle\underline{-2.5}$	$2.5\angle\underline{-2.5}$	$2.1\angle\underline{-2.3}$	$2.1\angle\underline{-2.3}$
$\underline{U}_u^a$	$0.83\angle\underline{-3.0}$	$0.83\angle\underline{-3.0}$	$0.45\angle\underline{-3.0}$	$0.45\angle\underline{-3.0}$	$0.7\angle\underline{-2.3}$	$0.7\angle\underline{-2.3}$	$0.9\angle\underline{-2.7}$	$0.9\angle\underline{-2.7}$
$\underline{U}_u^b$	$0.83\angle\underline{1.19}$	$0.83\angle\underline{1.19}$	$0.45\angle\underline{1.19}$	$0.45\angle\underline{1.19}$	$1.1\angle\underline{1.1}$	$1.1\angle\underline{1.1}$	$0.7\angle\underline{0.6}$	$0.7\angle\underline{0.6}$
$\underline{U}_u^c$	$0.83\angle\underline{-0.9}$	$0.83\angle\underline{-0.9}$	$0.45\angle\underline{-0.9}$	$0.45\angle\underline{-0.9}$	$0.5\angle\underline{-1.4}$	$0.5\angle\underline{-1.4}$	$0.2\angle\underline{-0.2}$	$0.2\angle\underline{-0.2}$
$\underline{U}_l^a$	$0.83\angle\underline{0.14}$	$0.83\angle\underline{0.14}$	$0.45\angle\underline{0.14}$	$0.45\angle\underline{0.14}$	$0.7\angle\underline{-0.9}$	$0.7\angle\underline{-0.9}$	$0.9\angle\underline{0.4}$	$0.9\angle\underline{0.4}$
$\underline{U}_l^b$	$0.83\angle\underline{-1.95}$	$0.83\angle\underline{-1.95}$	$0.45\angle\underline{-1.95}$	$0.45\angle\underline{-1.95}$	$1.1\angle\underline{-2.0}$	$1.1\angle\underline{-2.0}$	$0.7\angle\underline{-2.5}$	$0.7\angle\underline{-2.5}$
$\underline{U}_l^c$	$0.83\angle\underline{-4.05}$	$0.83\angle\underline{-4.05}$	$0.45\angle\underline{-4.05}$	$0.45\angle\underline{-4.05}$	$0.4\angle\underline{-4.5}$	$0.4\angle\underline{-4.5}$	$0.2\angle\underline{-3.4}$	$0.2\angle\underline{-3.4}$
$\underline{I}_u^a$	$0.475\angle\underline{0}$	$0.475\angle\underline{0}$	$1.44\angle\underline{0}$	$1.44\angle\underline{0}$	$2.0\angle\underline{0}$	$2.0\angle\underline{0}$	$1.4\angle\underline{0}$	$1.4\angle\underline{0}$
$\underline{I}_u^b$	$0.475\angle\underline{-2.09}$	$0.475\angle\underline{-2.09}$	$1.44\angle\underline{-2.09}$	$1.44\angle\underline{-2.09}$	$1.3\angle\underline{-3.8}$	$1.3\angle\underline{-3.8}$	$1.0\angle\underline{-3.9}$	$1.0\angle\underline{-3.9}$
$\underline{I}_u^c$	$0.475\angle\underline{-4.2}$	$0.475\angle\underline{-4.2}$	$1.44\angle\underline{-4.2}$	$1.44\angle\underline{-4.2}$	$1.3\angle\underline{-2.5}$	$1.3\angle\underline{-2.5}$	$1.0\angle\underline{-2.3}$	$1.0\angle\underline{-2.3}$
$\underline{I}_l^a$	$0.475\angle\underline{-3.14}$	$0.475\angle\underline{-3.14}$	$1.44\angle\underline{-3.14}$	$1.44\angle\underline{-3.14}$	$2.0\angle\underline{-3.1}$	$2.0\angle\underline{-3.1}$	$1.4\angle\underline{-3.1}$	$1.4\angle\underline{-3.1}$
$\underline{I}_l^b$	$0.475\angle\underline{1.05}$	$0.475\angle\underline{1.05}$	$1.44\angle\underline{1.05}$	$1.44\angle\underline{1.05}$	$1.3\angle\underline{-0.6}$	$1.3\angle\underline{-0.6}$	$1.0\angle\underline{-0.8}$	$1.0\angle\underline{-0.8}$
$\underline{I}_l^c$	$0.475\angle\underline{-1.05}$	$0.475\angle\underline{-1.05}$	$1.44\angle\underline{-1.05}$	$1.44\angle\underline{-1.05}$	$1.3\angle\underline{0.6}$	$1.3\angle\underline{0.6}$	$1.0\angle\underline{0.8}$	$1.0\angle\underline{0.8}$
$U_{u,l}^{jDC}$	0.5	0.5	0.5	0.5	0.5	0.5	0.5	0.5
$I_{u,l}^{aDC}$	-0.333	-0.333	-0.35	-0.35	-0.74	-0.74	-0.84	-0.84
$I_{u,l}^{bDC}$	-0.333	-0.333	-0.35	-0.35	0.21	0.21	-0.11	-0.11
$I_{u,l}^{cDC}$	-0.333	-0.333	-0.35	-0.35	0.21	0.21	-0.11	-0.11
I^{DC}	1	1	1.05	1.05	-0.32	-0.32	-1.02	-1.02

TABLE III
BALANCED AND FAULT COMPARISON (PART II)

Parameters	**AC grid condition**							
	Fault D		Fault E		Fault F		Fault G	
	Sim	Mod	Sim	Mod	Sim	Mod	Sim	Mod
$\underline{U}_g^a$	$0.3\angle\underline{0}$	$0.3\angle\underline{0}$	$0.8\angle\underline{0}$	$0.8\angle\underline{0}$	$0.3\angle\underline{0}$	$0.3\angle\underline{0}$	$0.6\angle\underline{0}$	$0.6\angle\underline{0}$
$\underline{U}_g^b$	$0.7\angle\underline{-1.8}$	$0.7\angle\underline{-1.8}$	$0.3\angle\underline{-2.1}$	$0.3\angle\underline{-2.1}$	$0.6\angle\underline{-1.8}$	$0.6\angle\underline{-1.8}$	$0.4\angle\underline{-2.5}$	$0.4\angle\underline{-2.5}$
$\underline{U}_g^c$	$0.7\angle\underline{-4.5}$	$0.7\angle\underline{-4.5}$	$0.3\angle\underline{-4.2}$	$0.3\angle\underline{-4.2}$	$0.6\angle\underline{-4.5}$	$0.6\angle\underline{-4.5}$	$0.4\angle\underline{-3.8}$	$0.4\angle\underline{-3.8}$
$\underline{I}_s^a$	$3.7\angle\underline{0}$	$3.7\angle\underline{0}$	$2.9\angle\underline{0}$	$2.9\angle\underline{0}$	$3.9\angle\underline{0}$	$3.9\angle\underline{0}$	$3.4\angle\underline{0}$	$3.4\angle\underline{0}$
$\underline{I}_s^b$	$2.7\angle\underline{-3.9}$	$2.7\angle\underline{-3.9}$	$4.8\angle\underline{-4.4}$	$4.8\angle\underline{-4.4}$	$3.1\angle\underline{-4.0}$	$3.1\angle\underline{-4.0}$	$2.7\angle\underline{-4.0}$	$2.7\angle\underline{-4.0}$
$\underline{I}_s^c$	$2.7\angle\underline{-2.3}$	$2.7\angle\underline{-2.3}$	$4.8\angle\underline{-1.9}$	$4.8\angle\underline{-1.9}$	$3.1\angle\underline{-2.2}$	$3.1\angle\underline{-2.2}$	$2.7\angle\underline{-2.2}$	$2.7\angle\underline{-2.2}$
$\underline{U}_u^a$	$0.5\angle\underline{-2.1}$	$0.5\angle\underline{-2.1}$	$0.8\angle\underline{-2.7}$	$0.8\angle\underline{-2.7}$	$0.6\angle\underline{-2.1}$	$0.6\angle\underline{-2.1}$	$0.8\angle\underline{-2.6}$	$0.8\angle\underline{-2.6}$
$\underline{U}_u^b$	$1.0\angle\underline{1.2}$	$1.0\angle\underline{1.2}$	$0.9\angle\underline{0.4}$	$0.9\angle\underline{0.4}$	$0.9\angle\underline{1.0}$	$0.9\angle\underline{1.0}$	$0.7\angle\underline{0.6}$	$0.7\angle\underline{0.6}$
$\underline{U}_u^c$	$0.5\angle\underline{-1.8}$	$0.5\angle\underline{-1.8}$	$0.3\angle\underline{-3.0}$	$0.3\angle\underline{-3.0}$	$0.3\angle\underline{-2.0}$	$0.3\angle\underline{-2.0}$	$0.0\angle\underline{-0.2}$	$0.0\angle\underline{-0.2}$
$\underline{U}_l^a$	$0.5\angle\underline{1.0}$	$0.5\angle\underline{1.0}$	$0.8\angle\underline{0.5}$	$0.8\angle\underline{0.5}$	$0.6\angle\underline{-1.0}$	$0.6\angle\underline{-1.0}$	$0.8\angle\underline{0.5}$	$0.8\angle\underline{0.5}$
$\underline{U}_l^b$	$1.0\angle\underline{-2.0}$	$1.0\angle\underline{-2.0}$	$0.9\angle\underline{-2.7}$	$0.9\angle\underline{-2.7}$	$0.9\angle\underline{-2.1}$	$0.9\angle\underline{-2.1}$	$0.7\angle\underline{-2.5}$	$0.7\angle\underline{-2.5}$
$\underline{U}_l^c$	$0.5\angle\underline{1.4}$	$0.5\angle\underline{1.4}$	$0.3\angle\underline{0.1}$	$0.3\angle\underline{0.1}$	$0.3\angle\underline{1.1}$	$0.3\angle\underline{1.1}$	$0.0\angle\underline{-3.4}$	$0.0\angle\underline{-3.4}$
$\underline{I}_u^a$	$1.9\angle\underline{0}$	$1.9\angle\underline{0}$	$1.5\angle\underline{0}$	$1.5\angle\underline{0}$	$1.2\angle\underline{0}$	$1.2\angle\underline{0}$	$1.7\angle\underline{0}$	$1.7\angle\underline{0}$
$\underline{I}_u^b$	$1.3\angle\underline{-3.9}$	$1.3\angle\underline{-3.9}$	$2.4\angle\underline{-4.4}$	$2.4\angle\underline{-4.4}$	$1.6\angle\underline{-4.0}$	$1.6\angle\underline{-4.0}$	$1.4\angle\underline{-4.0}$	$1.4\angle\underline{-4.0}$
$\underline{I}_u^c$	$1.3\angle\underline{-2.3}$	$1.3\angle\underline{-2.3}$	$2.4\angle\underline{-1.9}$	$2.4\angle\underline{-1.9}$	$1.6\angle\underline{-2.2}$	$1.6\angle\underline{-2.2}$	$1.4\angle\underline{-2.2}$	$1.4\angle\underline{-2.2}$
$\underline{I}_l^a$	$1.9\angle\underline{-3.1}$	$1.9\angle\underline{-3.1}$	$1.5\angle\underline{-3.1}$	$1.5\angle\underline{-3.1}$	$1.9\angle\underline{-3.1}$	$1.9\angle\underline{-3.1}$	$1.7\angle\underline{-3.1}$	$1.7\angle\underline{-3.1}$
$\underline{I}_l^b$	$1.3\angle\underline{-0.9}$	$1.3\angle\underline{-0.9}$	$2.4\angle\underline{-1.3}$	$2.4\angle\underline{-1.3}$	$1.6\angle\underline{-0.9}$	$1.6\angle\underline{-0.9}$	$1.4\angle\underline{-0.9}$	$1.4\angle\underline{-0.9}$
$\underline{I}_l^c$	$1.3\angle\underline{0.8}$	$1.3\angle\underline{0.8}$	$2.4\angle\underline{1.3}$	$2.4\angle\underline{1.3}$	$1.6\angle\underline{0.9}$	$1.6\angle\underline{0.9}$	$1.4\angle\underline{0.9}$	$1.4\angle\underline{0.9}$
$U_{u,l}^{jDC}$	0.5	0.5	0.5	0.5	0.5	0.5	0.5	0.5
$I_{u,l}^{aDC}$	-0.46	-0.46	-0.86	-0.86	-0.48	-0.48	-0.94	-0.94
$I_{u,l}^{bDC}$	0.47	0.47	0.25	0.25	0.44	0.44	-0.03	-0.03
$I_{u,l}^{cDC}$	0.47	0.47	0.25	0.25	0.44	0.44	-0.03	-0.03
I^{DC}	0.48	0.48	-0.37	-0.37	0.41	0.41	-1	-1